

Alkanethiolate-Protected Palladium Nanoparticles

Shaowei Chen,* Kui Huang, and Jaime A. Stearns†

Department of Chemistry and Biochemistry, Southern Illinois University,
Carbondale, Illinois 62901-4409

Received October 5, 1999. Revised Manuscript Received November 15, 1999

The synthesis and characterization of stable nanometer-sized alkanethiolate-protected palladium particles are described. The particles were synthesized in a biphasic system, and the formation appeared to involve a dynamic process, where initially larger particles were quickly formed, followed by decomposition into smaller and more stable particles. The solution color was found to change concurrently. With varied synthetic conditions, the particle size was found to vary and fall mainly within the size range of 1–5 nm in diameter with modest dispersity as determined by transmission electron microscopy. UV–vis spectroscopic measurements showed a Mie scattering profile, but no well-defined surface–plasmon resonance. FTIR studies indicated that the monolayers became more ordered with longer chain lengths of the protecting alkanethiolates. Electrochemical studies exhibited the solution-phase Coulomb staircase charging of the particle double layers, analogous to the observations with gold particles, where the peak spacings corresponded to a (sub)attofarad capacitance for the palladium particles.

Introduction

Recently there has been an extensive interest in the development of new methodologies for the fabrications of nanometer-sized materials.^{1,2} The emergence of nanoscience is largely attributed to the unique properties arising from the material dimensions that are of the order of the electron mean-free path (“quantum effects”), and motivated by their diverse application potentialities unexplored before.^{1,2} Among these, some research efforts have been directed toward the synthesis of palladium nanoclusters, partly because of the important roles played by palladium in catalysis where the catalytic activity has been found to be very sensitive to the particle size, shape, surrounding media, etc.^{3–10} Pd

colloidal particles have been prepared by a variety of techniques, including sonochemical reduction,³ chemical liquid deposition,⁴ refluxing alcohol reduction,⁵ decomposition of organometallic precursors,⁶ hydrogen reduction,⁷ and electrochemical deposition,^{8,9} where, in general, the particles were formed by the reduction of the metal ions in the presence of stabilizers or heterogeneous supports such as polymers or electrode surfaces, and the particle size, typically in the nanometer regime, could be controlled by varying the reaction conditions. More recently, Ulman et al. briefly reported a one-phase synthetic procedure to generate alkanethiolate-protected palladium nanoparticles using superhydride as the reducing agent.¹⁰

Monolayer-protected nanoclusters (MPC) are of particular interest in that they exhibit great stability in both solution and dry forms, in contrast to conventional colloidal particles.¹ In addition, MPCs in solutions behave as individual molecular entities, emerging as new artificial molecules. In this report, we describe the synthesis and characterizations of alkanethiolate-protected palladium nanoclusters using the biphasic system that was originally adopted for the synthesis of nanometer-sized gold clusters stabilized by a mercaptoorganic monolayer.^{11–13} We opt to employ the same route, partly because we are interested in studying the effects of different metal cores on the final particle size

* To whom correspondence should be addressed. Telephone: (618) 453-2895. Fax: (618) 453-6408. E-mail: schen@chem.siu.edu.

† Undergraduate summer researcher.

(1) (a) Schmid, G. *Clusters and Colloids: From Theory to Applications*; VCH: New York, 1994. (b) Haberland, H., Ed. *Clusters of Atoms and Molecules*; Springer-Verlag: New York, 1994. (c) Turton, R. *The Quantum Dot: A Journey into the Future of Microelectronics*, Oxford University Press: New York, 1995. (d) Hayat, M. A., Ed. *Colloidal Gold: Principles, Methods, and Applications*, Vol. 1, Academic Press: New York, 1989.

(2) See also all the review articles in the Feb 16, 1996, issue of *Science*.

(3) (a) Mizukoshi, Y.; Okitsu, K.; Maeda, Y.; Yamamoto, T. A.; Oshima, R.; Nagata, Y. *J. Phys. Chem. B* **1997**, *101*, 7033. (b) Dhas, N. A.; Gedanken, A. *J. Mater. Chem.* **1998**, *8*, 445.

(4) Galo Cardenas T.; Cesar Munoz, D.; Viviana Vera, L. *Bol. Soc. Chil. Quim.* **1996**, *41*, 235.

(5) (a) Mayer, A. B. R.; Mark, J. E. *Macromol. Rep.* **1996**, *A33* (Suppl. 7 and 8), 451. (b) Mayer, A. B. R.; Mark, J. E. *Colloid Polym. Sci.* **1997**, *275*, 333. (c) Teranishi, T.; Miyake, M. *Chem. Mater.* **1998**, *10*, 594.

(6) Giorgio, S.; Chapon, C.; Henry, C. R. *Langmuir* **1997**, *13*, 2279.

(7) (a) Schmid, G.; Harms, M.; Malm, J.-O.; Bovin, J.-O.; van Ruitenbeck, J.; Zandbergen, H. W.; Fu, W. T. *J. Am. Chem. Soc.* **1993**, *115*, 2046. (b) Schmid, G. *Chem. Rev.* **1992**, *92*, 1709. (c) Schmid, G. *Polyhedron* **1988**, *7*, 2321.

(8) (a) Reetz, M. T.; Quaiser, S. A. *Angew. Chem., Int. Ed. Engl.* **1995**, *34*, 2240. (b) Reetz, M. T.; Helbig, W. *J. Am. Chem. Soc.* **1994**, *116*, 7401.

(9) (a) Li, F.; Zhang, B.; Dong, S.; Wang, E. *Electrochim. Acta* **1997**, *42*, 2563. (b) Lu, D.; Tanaka, K. *J. Phys. Chem. B* **1997**, *101*, 4030.

(10) Yee, C. K.; Jordan, R.; Ulman, A.; White, H.; King, A.; Rafailovich, M.; Sokolov, J. *Langmuir* **1999**, *15*, 3486.

(11) Brust, M.; Walker, M.; Bethell, D.; Schiffrin, D. J.; Whyman, M. *J. Chem. Soc., Chem. Commun.* **1994**, 801.

(12) (a) Hostetler, M. J.; Murray, R. W. *Curr. Opin. Colloid Interface Sci.* **1997**, *2*, 42. (b) Hostetler, M. J.; Wingate, J. E.; Zhong, C.-J.; Harris, J. E.; Vachet, R. W.; Clark, M. R.; Londono, J. D.; Green, S. J.; Stokes, J. J.; Wignall, G. D.; Glish, G. L.; Porter, M. D.; Evans, N. D.; Murray, R. W. *Langmuir* **1998**, *14*, 17.

(13) Chen, S.; Murray, R. W. *Langmuir* **1999**, *15*, 682.

and size dispersity, which might shed some light on the nanoparticle growth mechanism.

Previous work on gold MPCs synthesized by using the above route¹¹ has revealed that the particle size can be easily controlled by the experimental parameters such as reaction media, solution temperature, thiol ligand structures, thiol:metal ratio, etc.^{12–18} Compared to other routes utilizing less potent reducing agents, such as citrate,^{1d} this phase-transfer procedure using borohydride as the reducing agent generates much smaller particles with a typical size range of 1–5 nm in diameter.^{11–18} With the passivation of an organic dielectric layer, gold MPCs exhibit (sub)attofarad (aF) capacitance that can be easily evaluated by solution electrochemistry.^{19,20} In solutions of relatively monodisperse MPCs, electrochemical ensemble Coulomb staircase charging has been observed, which was interpreted on the basis of the quantized charging of the double layers of the diffusive MPCs.¹⁹ A size-dependent transition of the charging characteristics from those of redox chemistry to those of bulk charging has also been observed.¹⁹

Understandably, MPC properties are dependent upon both the core metals and the protecting layers. Therefore, a quite significant part of the current research effort has been directed toward developing synthetic protocols for making nanoparticles of different metal elements. In combination with the surface chemistry involved in the functionalization of particle protecting monolayers, these new members of the rapidly growing nanoparticle family are anticipated to provide more insight in the tailoring of nanoscale advanced material properties. Here, we describe the synthesis of palladium nanoclusters stabilized by an alkanethiolate monolayer, with a focus on the growth dynamics and experimental manipulations of particle structures, followed by preliminary spectroscopic and electrochemical characterizations. Comparisons with gold MPCs will also be discussed.

Experimental Section

Materials. Palladium chloride (PdCl₂, 96%, ACROS), tetra-*n*-octylammonium bromide (TOABr, 98%, Aldrich), tetra-*n*-butylammonium perchlorate (TBAP, 99%, Aldrich), hydrochloric acid (HCl, Fisher), sodium borohydride (NaBH₄, 99+%, ACROS), *n*-hexanethiol (C6SH, 96%, Aldrich), and all solvents (from Fisher) were used as received. Water was supplied with a Barnstead Nanopure water system (18.3 MΩ).

ric acid (HCl, Fisher), sodium borohydride (NaBH₄, 99+%, ACROS), *n*-hexanethiol (C6SH, 96%, Aldrich), and all solvents (from Fisher) were used as received. Water was supplied with a Barnstead Nanopure water system (18.3 MΩ).

Particle Synthesis. The palladium nanoparticles were synthesized in a biphasic system.¹¹ In a typical reaction, 0.17 g (1 mmol) of PdCl₂ was dissolved in 50 mL of ~0.5 M HCl under vigorous stirring. A total of 80 mL of toluene with 1.1 g of TOABr was then added into this solution, where the bright orange/red Pd(II) was transferred from the aqueous phase to the toluene phase. The aqueous phase was then removed, and a calculated amount of C6SH was injected into the toluene solution (depending on the desired C6SH:Pd ratio). The solution was stirred for about 20 min, and then 0.39 g of NaBH₄ in 20 mL of H₂O was added quickly into the solution, where, after a few seconds delay, the solution color changed rapidly from orange/red to dark green/black, indicating the formation of palladium particles, akin to the case of gold nanoparticles where the color changed from bright red to dark brown/black.¹¹ Here it should be noted that the resulting particles were referred to by their specific experimental conditions, for instance, C6Pd (rt, 1/2×) refers to the particles synthesized in a solution kept at room temperature with a molar ratio C6S:Pd = 1:2; while for C6Pd (0 °C, 3×), the solution was kept at 0 °C prior to the addition of NaBH₄, with C6S:Pd = 3:1.

The solution was under vigorous stirring typically for ~20 min before the toluene part was collected. Solvent was then removed under reduced pressure with a rotary evaporator, and the resulting samples were thoroughly rinsed with ethanol and acetone to remove excessive thiols and other reaction byproducts. The particles appeared to be very stable and shared the solubility properties of the gold counterparts, very soluble in apolar solvents (e.g., toluene, benzene, hexane, chloroform, etc.) but not in polar solvents (e.g., alcohols, acetone).

If the aqueous phase was not separated and the synthetic solution was allowed to be under stirring in air without interruption, the solution color was found to gradually change back to orange/red. After ~90 min, the solution would be almost completely opaquely orange/red. This might indicate the decomposition of the initially formed Pd particles. Detailed discussions can be found in the next section.

Spectroscopic Studies. ¹H NMR spectroscopy was carried out with a Varian 300 VX NMR spectrometer with concentrated particle solutions in benzene-*d*₆. Only two broad peaks for the methyl and methylene protons were observed, where the absence of sharp lines in the NMR spectra indicated that the samples were spectroscopically clean. UV–vis spectroscopy was performed with a Unicam ATI UV–vis spectrometer with a resolution of 2 nm.

Vibrational spectroscopic study was carried out with a Nicolet 960 FTIR spectrometer. A thick film of samples was prepared on a KBr plate by dropcasting the corresponding solutions in CH₂Cl₂, which was then further dried in a N₂ stream. Data were collected from 100 scans (with a resolution of 4 cm⁻¹) and background corrected.

Transmission Electron Microscopy (TEM). TEM studies were performed with a Hitachi 7100 TEM (100 keV) which is also equipped for energy dispersive X-ray (EDX) analysis (NORAN Voyager III). Samples were prepared by dropcasting a particle solution in hexane with a typical concentration of ~1 mg/mL onto a 400 mesh Formvar-coated copper grid. For samples prepared directly from the original synthetic (toluene) solution, carbon-coated grids were used. Phase-contrast TEM micrographs were typically taken at three different spots of the grids with 300–500K magnification. Particle size analysis was then performed by digitizing the micrographs with Scion, from which the histograms of the particle size distributions were generated. Twin or particle aggregates were removed manually prior to size measurements.

Electrochemistry. Electrochemical measurements were carried out with a BAS 100B/W Electrochemical workstation. A polycrystalline gold disk electrode (0.076 cm²) sealed in a glass tubing was used as the working electrode, a Ag/AgCl as the reference and a Pt coil as the counter electrode. Prior to

(14) Wuelfing, W. P.; Gross, S. M.; Miles, D. T.; Murray, R. W. *J. Am. Chem. Soc.* **1998**, *120*, 12696.

(15) (a) Templeton, A. C.; Chen, S.; Gross, S. M.; Murray, R. W. *Langmuir* **1999**, *15*, 66. (b) Schaaff, T. G.; Knight, G.; Shafiqullin, M. N.; Borkman, R. F.; Whetten, R. L. *J. Phys. Chem. B* **1998**, *102*, 10643.

(16) Whetten, R. L.; Khoury, J. T.; Alvarez, M. M.; Murthy, S.; Vezmar, I.; Wang, Z. L.; Stephens, P. W.; Cleveland, C. L.; Luedtke, W. D.; Landman, U. *Adv. Mater.* **1996**, *8*, 428.

(17) Leff, D. V.; Ohara, P. C.; Heath, J. R.; Gelbert, W. M. *J. Phys. Chem.* **1995**, *99*, 7036.

(18) Schaaff, T. G.; Shafiqullin, M. N.; Khoury, J. T.; Vezmar, I.; Whetten, R. L.; Cullen, W. G.; First, P. N.; Gutiérrez-Wing, C.; Ascensio, J.; Jose-Yacamán, M. *J. Phys. Chem. B* **1997**, *101*, 7885.

(19) (a) Ingram, R. S.; Hostetler, M. J.; Murray, R. W.; Schaaff, T. G.; Khoury, J.; Whetten, R. L.; Bigioni, T. P.; Guthrie, D. K.; First, P. N. *J. Am. Chem. Soc.* **1997**, *119*, 9279. (b) Chen, S.; Ingram, R. S.; Hostetler, M. J.; Pietron, J. J.; Murray, R. W.; Schaaff, T. G.; Khoury, J. T.; Alvarez, M. M.; Whetten, R. L. *Science* **1998**, *280*, 2098. (c) Chen, S.; Murray, R. W.; Feldberg, S. W. *J. Phys. Chem. B* **1998**, *102*, 9898. (d) Hicks, J. F.; Templeton, A. C.; Chen, S.; Sheran, K. M.; Jasti, R.; Murray, R. W.; Debord, J.; Schaaff, T. G.; Whetten, R. L. *Anal. Chem.* **1999**, *71*, 3703.

(20) (a) Green, S. J.; Stokes, J. J.; Hostetler, M. J.; Pietron, J. J.; Murray, R. W. *J. Phys. Chem. B* **1997**, *101*, 2663. (b) Green, S. J.; Pietron, J. J.; Stokes, J. J.; Hostetler, M. J.; Vu, H.; Wuelfing, W. P.; Murray, R. W. *Langmuir* **1998**, *14*, 5612.

electrochemical measurements, the Au electrode was polished with 0.05 μm $\alpha\text{-Al}_2\text{O}_3$ slurries (Buerhler), followed by extensive rinsing with dilute H_2SO_4 , Nanopure water, ethanol, and acetone consecutively.

Results and Discussion

In this section, we begin with a study of the reaction dynamics of palladium particle formation by using transmission electron microscopy (TEM), followed by TEM measurements of the particle core size and size distribution with varied experimental conditions. Results from spectroscopic and electrochemical measurements of the Pd particle solutions will also be presented, along with comparisons with those of the gold counterparts.

Growth Dynamics. As described in the Experimental Section, upon the addition of reducing agent (NaBH_4), the synthetic solution exhibited a drastic color change after an induction time of a few seconds: from orange/red to dark green/black. This indicated the formation of palladium particles, akin to the reaction of gold MPC formation.^{11–18} However, the solution color was found to slowly change back to orange/red if the solution was allowed to be stirred under ambient conditions for a fairly long period of time (e.g., 90 min), suggesting that the initially produced particles were not stable and decomposed back to Pd ionic complexes and/or very fine palladium particles. Therefore, to investigate the intrinsic details involved in this dynamic process, we carried out TEM measurements by, at varied reaction times, dropcasting the original synthetic solution onto a carbon-coated copper grid. Figure 1 shows the TEM micrographs of C6Pd (0 °C, 3 \times) particles at varied reaction times, where one can see that at the very early stage of the reaction, the particles were quite big: at 7.5 min, 5.46 ± 2.39 nm; and at 15 min, 6.48 ± 1.50 nm. However, at 30 min, the particle size decreased quite significantly to only 2.31 ± 0.83 nm, and at 60 min, 2.98 ± 0.88 nm. Furthermore, the core size dispersity also shows a decrease from initially about 44% to 30% at 60 min. Figure 2 depicts the corresponding growth dynamics, where one can see that within the error bars of the size dispersity, the Pd particles appeared to undergo a rapid nucleation in the first 15 min, which then decomposed into much smaller sizes, reaching a more stable stage in the next 60 min or so. At longer reaction times (>90 min), the solution color changed completely back to (opaquely) orange/red, and TEM revealed featureless images.

The observed growth dynamics of palladium MPCs is very different from that of the gold counterparts. In our previous study of the reaction dynamics of gold nanoparticles,²¹ it was found that the gold particles (i) were formed rather rapidly, within seconds after the addition of the reducing agent; (ii) showed a slight increase of the core size within the first few minutes; and (iii) afterward, only experienced modest fluctuation in size and size distribution in the time span up to 5 days. This observed discrepancy of reaction dynamics might, at least in part, be attributed to the variation of the metal–metal and metal–sulfur bonding strengths, where the dynamic behavior of Pd MPCs might be a direct

consequence of the much weaker Pd–Pd and Pd–S bonding interactions.²²

At the moment, it is somewhat unclear why the Pd particles would eventually “disappear”, presumably decomposed into extremely fine particles, and/or reoxidized into ionic complexes, as the solution color strongly suggested. However, the effect of oxygen seems to be excluded,^{7b} as in a control experiment (also under ambient conditions) where no thiols were initially added, i.e., palladium “naked” particles were produced, the solution turned dark brown/black upon the addition of NaBH_4 , and the color remained unchanged for more than 24 h of stirring, even after subsequent addition of alkanethiols. More detailed studies of the identifications of reaction byproducts and their interactions with Pd particles are currently underway which are desired to better address the observed reaction dynamics.

In short, it appears that the growth dynamics of Pd MPCs can be summarized into three stages: (i) in the first 15 min, rapid nucleation into big particles after a few seconds of induction time; (ii) breakup into smaller and more stable particles in the following 60 min; (iii) at a longer reaction time (~ 90 min), no visible features by TEM, presumably due to particle decomposition.

TEM Study. In light of the above study, for all particle synthesis, the reaction was terminated at ~ 20 min after the addition of NaBH_4 . It should be mentioned that after solvent removal, the particles were collected and purified, and the black color of the powdery samples remained unchanged either in solution or dry forms. Here we varied the experimental parameters and investigated their effects on the resulting particle size and size dispersity. Figure 3, parts A and B, shows two representative TEM micrographs of C6Pd MPCs with varied synthetic conditions, where insets show the corresponding core size distributions. The overall summary is listed in Table 1. One can see that in general, the particles are quite small, within the size range of 1–5 nm, with the majority between 2 and 4 nm and a modest dispersity (about 13–30%). The relatively small dispersity of the palladium particle sizes, compared to that of the gold counterparts synthesized under similar experimental conditions,^{12b} indicates that the Pd cores are energetically more selective. Previous work on silver MPCs²³ also shows smaller size dispersity than the gold counterparts.

Figure 3D shows the variation of C6Pd particle size with C6S: Pd ratio at two different temperatures (0 °C and room temperature), where one can see that the particle size distribution appears to be more sensitive to the reaction solution temperature (from 0 °C to room temperature) than to the C6SH: Pd ratio (from 3 \times to 1/6 \times), within the size deviation. For instance, only very slight change of the particle mean diameter is observed with the C6S: Pd ratio ranging from 1 to 1/6 at room temperature; similar observation can also be found at 0 °C with C6S: Pd varied from 3 to 1. However, when solution temperature changes from 0 °C to room temperature, the particle size decreases from 3.36 to 2.52

(22) See, for instance: *CRC Handbook of Chemistry and Physics*, 76th ed.; Lide, D. R., Ed.; CRC Press: Baton Rouge, 1995.

(23) (a) Collier, C. P.; Saykally, R. J.; Shiang, J. J.; Henrichs, S. E.; Heath, J. R. *Science* **1997**, *277*, 1978. (b) Harfenist, S. A.; Wang, Z. L.; Alvarez, M. M.; Vezmar, I.; Whetten, R. L. *J. Phys. Chem.* **1996**, *100*, 13904.

(21) Chen, S.; Templeton, A. C.; Murray, R. W. *Langmuir* **2000**, *16*, in press.

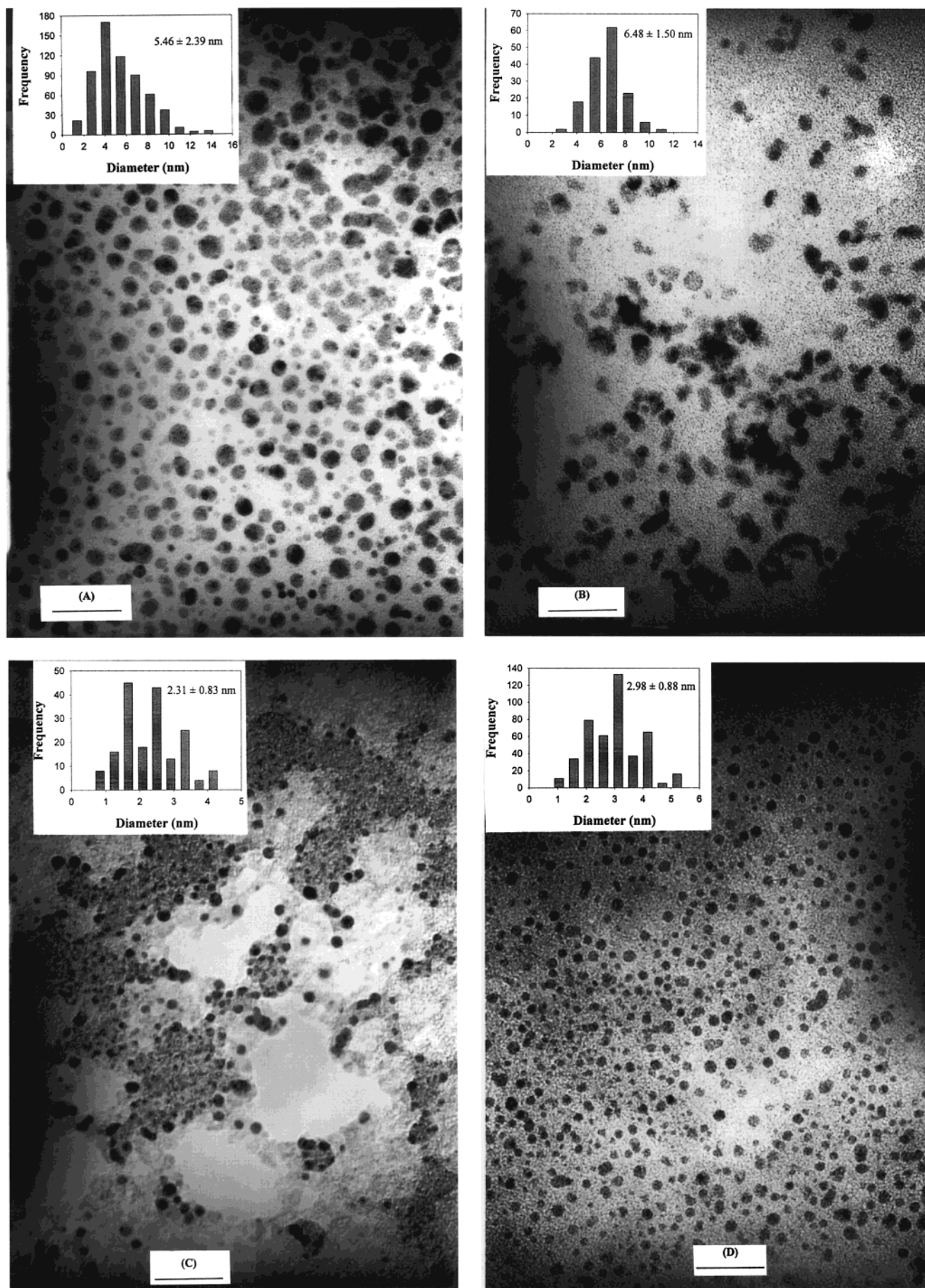


Figure 1. TEM micrographs of C6Pd (0 °C, 3x) clusters at varied reaction times: (A) 7.5 min, (B) 15 min, (C) 30 min, and (D) 60 min. Insets show the corresponding size histograms. Scale bars are (A) 33 nm, (B) 33 nm, (C) 20 nm, and (D) 25 nm.

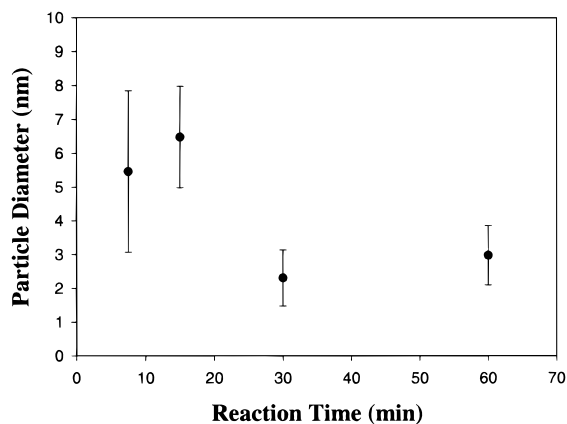


Figure 2. Pd particle growth dynamics. Data were obtained from Figure 1.

nm at C6S:Pd = 1. At first glance, this trend is rather unexpected and appears to be counterintuitive, as previous studies^{12b} on gold MPCs have shown that with increasing solution temperature, the particles increased in size. In addition, the average size of gold MPCs was very sensitive to the initial RS:Au ratio as well, where the particle mean diameter was found to increase from 1.73 nm (0 °C, 3×) to 4.40 (rt, 1/6×) (Table 1). This, again, strongly suggests that the growth mechanism for monolayer-protected nanoclusters might vary depending upon the nature of the specific metals. This is also consistent with the observation of a relatively long induction time in Pd particle formation compared to the gold counterparts where the solution color changed almost instantly upon the addition of the reducing agent (NaBH₄).

On the other hand, the particle size and size dispersity were found to be quite insensitive to the variation of chain lengths of the protecting alkanethiol ligands (not shown), for instance, from *n*-butanethiol (C4SH) to *n*-octadecanethiol (C18SH). This is similar to the earlier observation with gold particles.^{12b}

The above studies indicate that for palladium particles, the final particle size and size distribution might be mainly governed by the dynamics involved in core formation, and the reaction kinetics appears to be very sensitive to solution temperature. In contrast, for gold particles, the termination of particle growth by the passivation process appears to be the determining step in final particle size distribution, since the cores are relatively more stable (in consistence with the stronger Au–Au and Au–S bonds, as mentioned earlier).²¹

On the other hand, chains of particles in the TEM pictures can be seen for both the hexanethiolate–MPCs (for instance, see Figure 3B) and the “naked” particles (Figure 3C). These observations are ascribed to the bilayerlike structures formed by similar-size particles, where the top layer sits on the 2-fold saddle rather than the 3-fold hollow sites, probably due to the balance of electrostatic repulsion and dispersion interactions between neighboring particles.^{13,24} This is consistent with the relatively modest size dispersity, where the size histograms of the Pd MPCs synthesized here appear to be monomodal (Figure 3, insets). Also, the closest edge-

to-edge distance between neighboring particles roughly equals to the fully extended chain length of a single hexanethiolate (~0.8 nm), suggesting possible intercalation of the neighboring particle protecting monolayers.¹²

Spectroscopic Studies. Nanometer-sized metal clusters exhibit unique optical properties.²⁵ For instance, Au, Ag, and Cu nanoparticles exhibit a strong surface-plasmon resonance that is superimposed onto the exponential-decay Mie-scattering spectra.^{12,25} However, for nanometer-sized Pd particles, the absorption profile does not feature a well-defined surface-plasmon band; instead, for particles within the size range obtained above, only the Mie scattering spectra can be observed.²⁵ Figure 4 shows two representative spectra for the C6Pd (rt, 1×) and the “naked” Pd particles in toluene.²⁶ The absorption peak at ~320 nm observed with the original synthetic solution of “naked” Pd particles was ascribed to unreacted Pd complexes.

On the other hand, the structures and conformations of the protecting mercapto monolayers on nanoparticle core surfaces have been examined by vibrational spectroscopy.²⁷ Table 2 lists the band positions for the symmetric (d⁺) and antisymmetric (d⁻) C–H stretches of the methylene units for a series of RS:Pd (rt, 1×) particles with varied chain lengths of alkanethiols (the overall particle core size and size dispersity were similar, vide ante). These two bands have been used as a sensitive indicator for the ordering of the alkyl chains. One can see that with longer alkyl chain lengths, these two bands shifted to slightly lower energy, indicating a more ordered structure of the monolayer. For instance, for *n*-butanethiolate (C4), d⁺ lies at 2856 cm⁻¹ and d⁻ at 2925 cm⁻¹; whereas for *n*-octadecanethiolate (C18), they are found at 2851 and 2922 cm⁻¹, respectively. This is consistent with earlier studies on alkanethiolate-protected gold particles.²⁷

Electrochemical Measurements. Previously, it has been found that Au MPCs behave as diffusive nanoelectrodes in solutions,²⁰ and discrete electron charging to the MPC double-layer capacitance can be observed with solutions of relatively monodisperse particles.¹⁹ Voltammetrically, multiple well-defined reversible waves are exhibited within the potential range of -1.0 to +1.0 V, each of which corresponds to a single-electron-transfer process.¹⁹ The potential spacing (ΔV) between consecutive charging steps can be expressed as

$$\Delta V = e/C_{\text{MPC}} \quad (1)$$

where e is the electronic charge and C_{MPC} is the particle (integrated) capacitance. By assuming a concentric configuration of the MPC monolayer and core, C_{MPC} can be expressed as

$$C_{\text{MPC}} = 4\pi\epsilon\epsilon_0(r/d)(r + d) \quad (2)$$

where r is the core radius, d the monolayer thickness, ϵ the monolayer dielectric constant, and ϵ_0 the permittivity of vacuum. It should be noted that, in this

(25) Creighton, J. A.; Eadon, D. G. *J. Chem. Soc., Faraday Trans. 1991*, 87, 3881.

(26) For much bigger particles (>10 nm), a rather well-defined and yet broad absorption band can be observed at around 412 nm.

(27) Hostetler, M. J.; Stokes, J. J.; Murray, R. W. *Langmuir* 1996, 12, 3612.

(24) Fink, J.; Kiely, C. J.; Bethell, D.; Shiffrin, D. J. *Chem. Mater.* 1998, 10, 922.

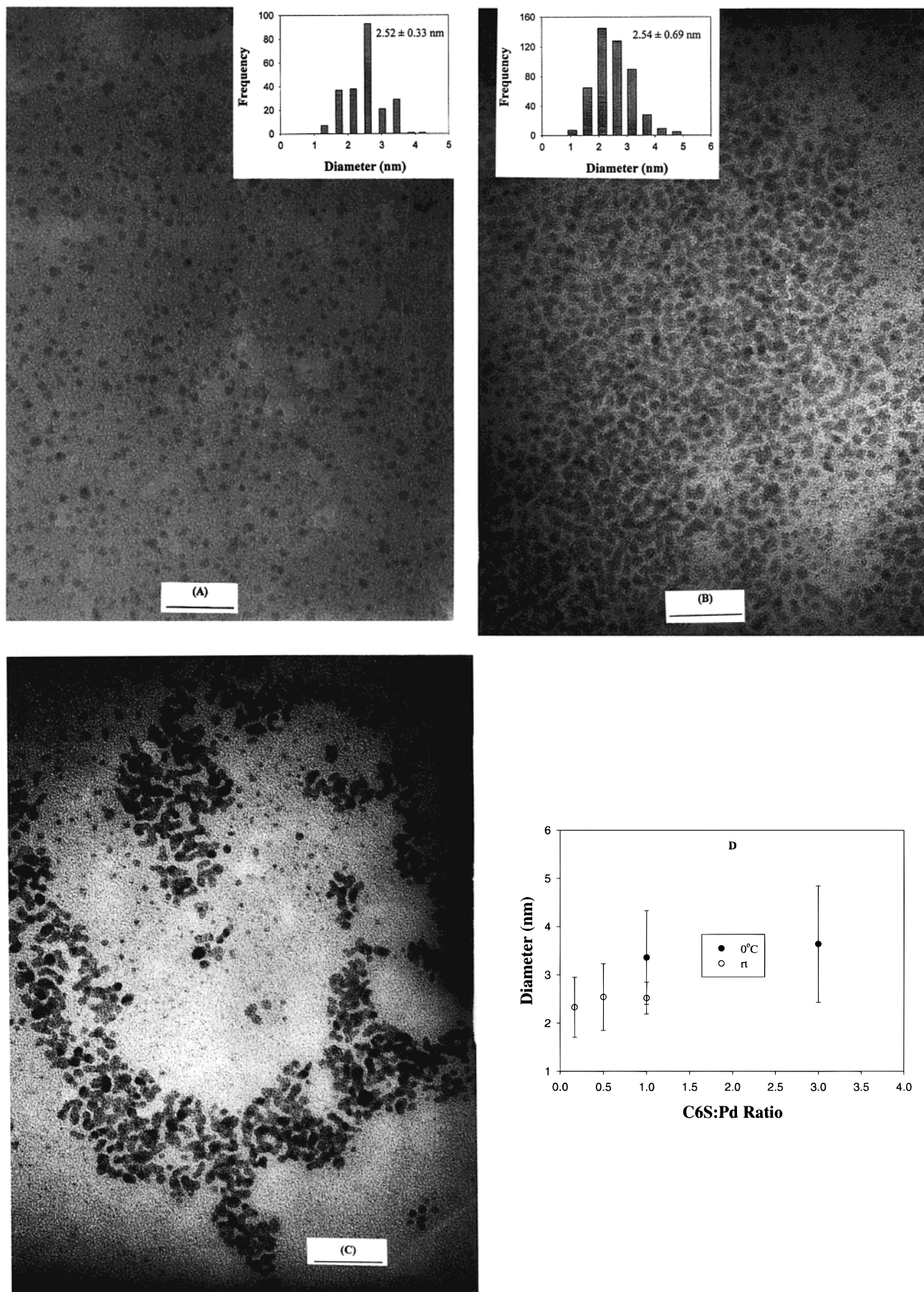


Figure 3. TEM micrographs of palladium clusters synthesized under varied experimental parameters: (A) C6Pd (rt, $1 \times$), (B) C6Pd (rt, $1/2 \times$), and (C) "naked" Pd (rt). Insets show the corresponding size histograms. Scale bars are (A) 20 nm, (B) 25 nm, and (C) 33 nm. (D) Variation of particle size and dispersity with C6S:Pd ratio at 0°C and room temperature.

Table 1. Size and Size Dispersity of *n*-Hexanethiolate-Protected Nanoclusters

	0 °C, 3×	0 °C, 2×	0 °C, 1×	rt, 1×	rt, 1/2×	rt, 1/6×	rt, "naked" ^e
Pd	3.64		3.36	2.52	2.54	2.33 ^c	4.34
MPC ^a	(1.21)		(0.97)	(0.33)	(0.69)	(0.62)	(1.29)
Au	1.73	1.92		2.00	2.40	4.40	~6.00
MPC ^b							

^a Numbers in parentheses denote dispersity. ^b From ref 12b. ^c Might be somewhat underestimated as the solubility was not as good as that of other samples. ^e No addition of thiols.

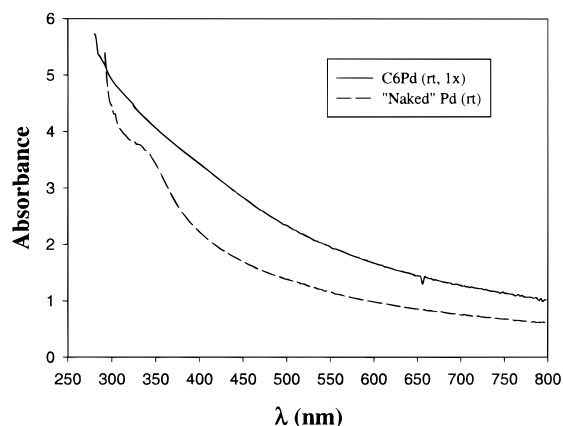


Figure 4. UV-vis spectra of C6Pd (rt, 1×) and "naked" Pd particles synthesized at room temperature. Solution concentrations ~0.6 mg/3 mL toluene.

Table 2. Symmetric (d⁺) and Antisymmetric (d⁻) C-H Stretches of the Methylene Units of a Series of Pd Particles (rt, 1×) Protected by Varied Alkanethiolates [CH₃(CH₂)_nS]

<i>n</i>	d ⁻ (cm ⁻¹)	d ⁺ (cm ⁻¹)
3	2925	2856
5	2918	2850
7	2923	2853
9	2923	2853
11	2921	2851
15	2922	2852
17	2922	2851

simplified approach that is based only on electrostatic interaction, the identity of the metal core is not taken into account; and previous work on discrete electron charging has been mainly focused on Au MPCs with few reports on other transition metal materials. It would be of great interest and fundamental importance to investigate the effect of core metals on the electron-transfer processes due to the possible influence of the variation of core electron energy distribution.

From the above TEM measurements, C6Pd (rt, 1×) particles exhibit the smallest core size dispersity, therefore these particles appear to be the most promising candidate that would demonstrate the electrochemical Coulomb staircase charging. Figure 5 shows the cyclic (A, CV) and differential pulse (B, DPV) voltammograms of the C6Pd (rt, 1×) MPC solution in 0.1 M TBAP in a mixed solvent of toluene and acetonitrile (2:1 v/v), where it can be seen that better resolved by DPV, there are multiple voltammetric waves between -0.7 and +0.5 V which appear to be quite reversible with the typical peak splitting (ΔE_p) less than 50 mV (Table 3). These behaviors are very similar to the observations of the ensemble Coulomb staircase charging with gold MPCs.^{13,19} From the potential spacing between consecu-

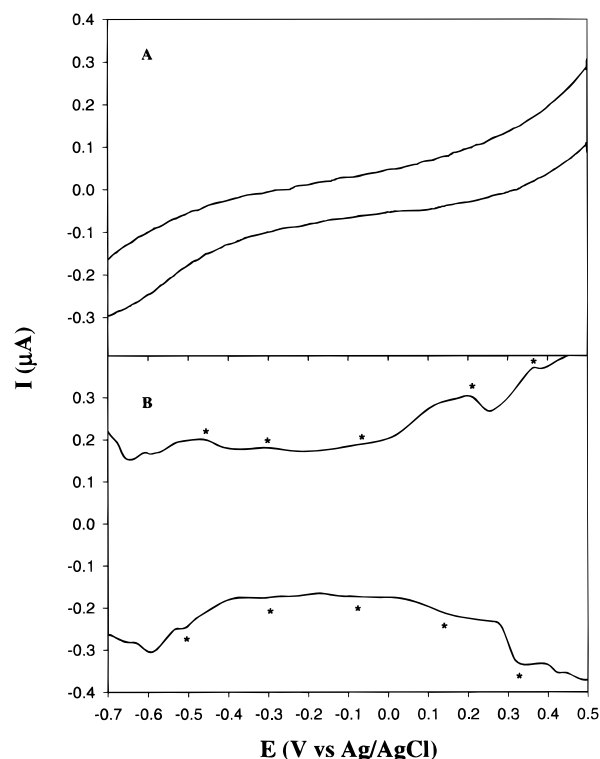


Figure 5. Cyclic (A, CV) and differential pulse voltammograms (B, DPV) of a solution of ~1 μM C6Pd (rt, 1×) clusters in 0.10 M TBAP in a binary mixture of toluene and acetonitrile (2:1 v/v): (A) potential sweep rate 30 mV/s and (B) potential sweep rate 10 mV/s, pulse amplitude 50 mV, pulse width 50 ms, and pulse period 200 ms. Asterisks indicate the DPV peak positions.

Table 3. Peak Potentials of the Coulomb Staircase Charging of C6Pd MPC Solutions in 0.1 M TBAP in Toluene and Acetonitrile (2:1 v/v), As Determined by DPV (data taken from Figure 5)

peak no.	E_{pa}^a (V)	E_{pc}^a (V)	$E^{0'}^a$ (V)	ΔE_p (V)	ΔV^b (V)
1	0.368	0.336	0.352	0.032	0.176
2	0.190	0.161	0.176	0.029	0.274
3	-0.096	-0.100	-0.098	0.004	0.210
4	-0.300	-0.315	-0.308	0.015	0.187
5	-0.470	-0.520	-0.495	0.050	0.135
6	-0.610	-0.650	-0.630	0.040	

^a All potentials vs Ag/AgCl reference. ^b Peak spacing between successive charging peaks.

tive charging peaks (~0.21 V), one can evaluate the C6Pd (rt, 1×) MPC capacitance (eq 1) to be about $C_{MPC} = 0.76$ aF. From eq 2, this corresponds to a dielectric constant of about 2.1 for the protecting monolayer, where the monolayer thickness is assumed to equal to the fully extended chain length of the C6S ligands. More detailed electrochemical studies of particles of varied sizes and monolayer structures are currently underway and will be reported in due course.

In this particular case, it appears that the quantized capacitance charging of the particle double layer is fairly insensitive to the core materials, which is probably due to the relatively big size of the particles. Previous studies have shown that for large particles, the charging behaviors can be best described as classical electrochemical charging of double layer capacitance where the main energetic barrier for electron transfer is due to electrostatic interactions.^{19c} However, for very small-

size particles where discrete energetic states start to emerge (manifested by the appearance of a HOMO–LUMO gap, for instance), additional energy barrier needs to be taken into account, and it should be anticipated that the specific metal core materials would have a significant effect on the electrochemical charging features.^{19c,28} Smaller and more monodisperse particles are needed to address this evolutionary effect.

Summary

The synthesis and characterization of palladium nanoparticles stabilized by alkanethiolate monolayers have been described. The palladium particles were found to undergo a dynamic growth process, with an initial rapid nucleation stage followed by decomposition into smaller and more stable particles. UV–vis spectroscopic studies showed a Mie scattering profile, but no well-defined surface-plasmon band. FTIR measure-

ments indicated that the alkanethiolate monolayers became more ordered with longer chain lengths. Electrochemical measurements exhibited solution-phase Coulomb staircase charging features, consistent with TEM studies where rather monodisperse particles were found. The behaviors observed here were quite similar to those with gold MPCs, where bulk charging characteristics dominated due to the relatively large particle cores. It is anticipated that the effects of metal core materials would be significant when the particle core size is sufficiently small, which causes additional energy barrier for electron charging to the particles.

Acknowledgment. This work was supported by Southern Illinois University at Carbondale through a start-up fund and the SIU Materials Technology Center. The authors are grateful to the SIU Center for Micro-Imaging and Analysis for technical assistance in TEM measurements, and Dr. B. C. Dave and M. Rao for providing access to the FTIR spectrometer.

(28) (a) Volokitin, Y.; Sinzig, J.; de Jongh, L. J.; Schmid, G.; Vargaftik, M. N.; Moiseev, I. I. *Nature* **1996**, *384*, 621. (b) Fritsche, H.-G. *Z. Phys. Chem.* **1995**, *191*, 219.

CM9906203